A Pipeline Inspection Robot with a Linkage Type Mechanical Clutch

Young-Sik Kwon, Bae Lee, In-Cheol Whang, and Byung-Ju Yi, *Member, IEEE*

bj@hanyang.ac.kr

Abstract—**This paper presents a new pipeline inspection robot with a linkage type mechanical clutch, which is designed for inspection of pipelines with 100mm diameter. This robot has three powered wheel chains each of which has a mechanical clutch. The mechanical clutch is designed by using a parallel linkage mechanism. The kinematic model of the pipeline inspection robot is driven and its proto type has been developed. The performance of this robot system is verified by both simulation and experimentation.**

I. INTRODUCTION

In-pipe robot mechanism, which has a long history of development in robotics, can be classified into several elementary forms according to the movement patterns. Therefore, many kinds of mechanisms have been developed like as wheel-type, inchworm-type, legged mobile-type, screw-type, crawler-type, PIG-type, and passive-type. Among them, wheel-type pipeline inspection robots were mostly popular [1]-[9]. During the latest 10 years, differential-drive type mechanisms have been studied intensively [10]-[12]. The differential-drive type usually has three powered chains. Controlling the speed of each chain independently, the robot is able to go through elbows and T-branches. Also, it has a large folding range compared with wheel type, screw-type, and PIG-type.

Recently, pipeline inspection robot systems with their diameter smaller than 100 mm have been focused, since the pipeline market smaller than 100mm is getting bigger. The diameters of most indoor pipelines are less than 100mm. Specifically, the clearance of indoor pipelines is directly related to the human health. Thus, cleaning and inspection of the in-house pipeline becomes an important issue.

Usually, pipeline inspection robot systems are composed of a robot mechanism, a communication system, a power supply, and a user interface. However, in order to apply it to real environment, some practical aspects such as easy user interface, safety, water proof, and retrieval function should be taken into account. Specifically, the retrieval function is crucial because the robot working inside the pipeline can be

out of order any time. Also the robot can be stuck in the pipeline by any reason during operation. In that case, the robot needs to be taken out of the pipeline by using some retrieval function. The concept of clutch is a good solution for realization of the retrieval function. There are two types of clutch; mechanical clutch and magnetic clutch. Usually, the mechanical clutch guarantees a strong power, but it is usually large-sized, heavy, and has a complex structure. On the contrary, the magnetic clutch is relatively small-sized, light, and has a simple structure, but it has a limitation in power.

Chang, *et al.* [13] designed a piezoelectric clutch mechanism, which contains a driving member connected to a DC motor and a driven member connected to a mechanical load. Maekawa, *et al.* [14] developed a non-contact load-responsive transmission. The absence of mechanical friction at the non-contact magnetic clutch resolves the problem concerning the wear and maintenance, the shock while switching the clutch is greatly reduced, and the actuator is protected from overloads by slippage at the magnetic clutch. Roh, *et al.* [15] employed a magnetic brake to connect or disconnect a power between the motor and the driving wheel mechanism. However, commonly such magnetic type clutch mechanisms are still too large and complex to apply to small-sized robots with less than 100mm diameter. Also the magnetic type has limitation in firm gripping.

In this paper, we introduce a new differential-drive type pipeline inspection robot with a compact-sized linkage-type mechanical clutch for 100 mm pipelines. The robot mechanism is designed using a parallel linkage so that it can provide two functions; the foldable characteristic and mechanical clutch. The foldable characteristic allows adaptation of the wheel mechanism to the wall inside the pipeline. The mechanical clutch function can be also realized by a parallel linkage design. This mechanical clutch is different from the typical large-sized mechanical clutch using two plates. Section II introduces the characteristics of the robot system. The kinematic analysis is presented in section III. We show the validity of this robot system by both simulation and experimentation in section IV. Lastly, we draw conclusion.

Y. S. Kwon is with the School of Electrical Engineering and Computer Science, Hanyang University, Korea. (e-mail: yskwon80@gmail.com)

Bae Lee is with the president of the Doobae system, Korea. (e-mail:doobae@dodbae.co.kr)

In-Cheol Whang is with the director of the Doobae system, Korea. (e-mail:hinch@com.ne.kr)

B. J. Yi is with the School of Electrical Engineering and Computer Science, Hanyang University, Korea. (corresponding author to provide phone: 82-31-400-5218; fax: 82-31-416-6416; e-mail: bj@hanyang.ac.kr)

II. CHARACTERISTICS OF ROBOT

A. The whole system and robot device

The robot system shown in the Fig. 1 consists of a control box and a robot device. Using the modularity, the robot device is separable from the control box.

The robot device consists of a main body, three wheel

chains, and three clutch wheel parts as shown in Fig. 2. The length of robot is 80mm and the exterior diameter is 100mm. Realization of the retrieval function through the mechanical linkage design is meaningful, because it removes the disadvantages of magnetic brakes such as slippage, limited power transmission, and limited size.

Fig. 1. The pipeline inspection robot system with a mechanical clutch.

This robot mechanism can be operated in two different modes; driving mode and retrieval mode. The driving mode represents that the robot is in motion, and the retrieval mode implies the state of retrieving the robot to the entrance location.

(a)

(b)
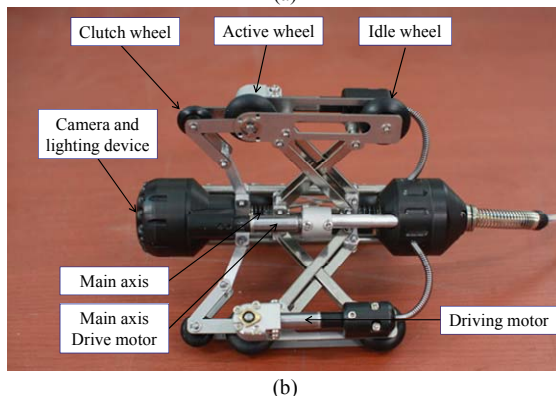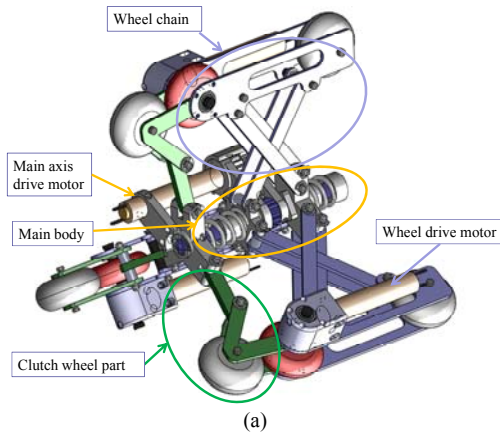
Fig. 2. The whole structure of the pipeline inspection robot system with a mechanical clutch : (a) The 3D model, (b) The developed robot.

For realization of both modes, we drive the robot device using three wheel drive motors and one main axis drive motor as shown in Fig. 2. Using the three wheel drive motors, we can control the forward and backward movement and the steering motion at the elbow. Switching from one mode to

another can be made by using the main axis drive motor.

B. *The main body*

As shown in Fig. 3, the main body consists of two nuts, two key sliders, two compression springs, and an axis drive motor. The nuts transfer power to each side of the main axis, the key slider slides along a groove of the nut and it is connected to the linkage of the wheel chain. The compression spring adapts to change of the outer diameter of the wheel chain. This design allows a foldable characteristic of the robot body. The main axis consists of a spur gear in the middle, a left-handed screw, and a right-handed screw. The power of the main axis drive motor is transferred to the main axis through the spur gear. The change of mode can be made by the main axis drive motor. Rotation of the main axis yields the translational motion of the screws. That results in displacement of the nuts as well as the key sliders at the same time.
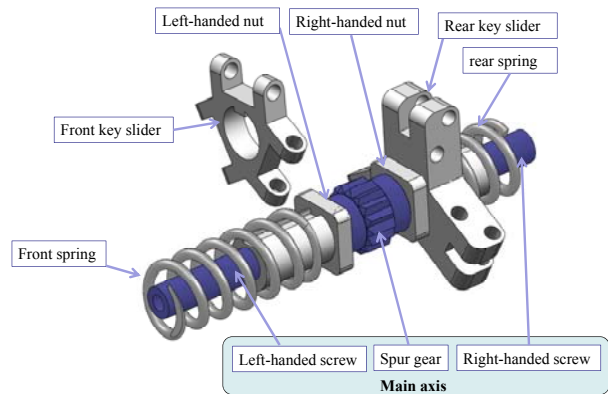
Fig. 3. The structure of the main body.

C. *The wheel chain and clutch part*

The left end of the main axis is connected to the clutch wheel part at the distal location of the screw. The wheel chain consists of a parallel linkage, a wheel drive motor (6ϕ), an active wheel, and an idle wheel. As shown in Fig. 2 and Fig. 4, each wheel chain is linked to the clutch part.

• 5-bar mechanism :
• 4-bar mechanism :
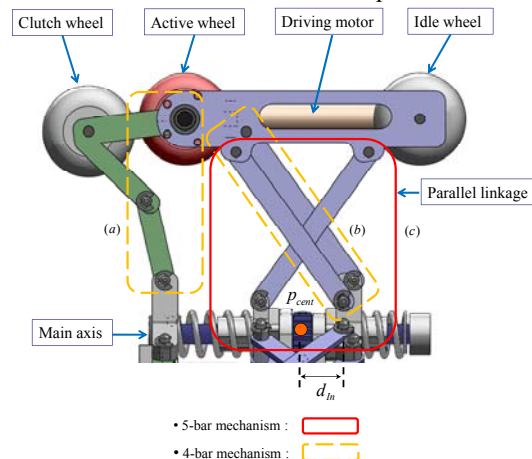
Fig. 4. The structure of the wheel chain and the clutch wheel.

The wheel drive motor drives the active wheel through a bevel gear power transmission. The clutch part consists of a clutch wheel and a linkage that connects the clutch wheel to the main axis. The clutch wheel is also an idle wheel. As shown in Fig. 6, the wheel chain is linked to the main axis by using four- and five-bar mechanisms. A parallelogram mechanism is employed to keep a horizontal posture of the wheel chain. The motion of the wheel chain is coupled to the motion of the clutch wheel through a four-bar that connects the main axis to the upper part of the wheel chain.

D. Driving and retrieval modes of the robot device

When the robot is being inserted into a pipeline, the outer diameter of the robot is adjusted by using the main axis drive motor. Fig. 5(a) denotes the state that the robot is being inserted into the pipeline in the driving mode, where two nuts are located in the middle. When the wheel of the robot passes through an irregular surface or a small bumper inside the pipeline, an external force is applied to the wheel chain. As a result, the key sliders connected to the wheel chain behave like Fig. 5(b). Compression springs located at both sides of the main axis play the role of shock absorption. When the robot goes over the bumper part, the key slider goes back to the state of Fig. 5(a) due to the restoring force of the compression spring.
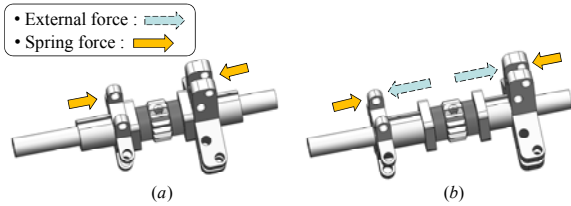
Fig. 5. The driving mode.

Fig. 6 shows the retrieval mode. Activating the main axis drive motor, the initial configuration of the main axis is set up as this configuration where the two nuts are farther apart. As a result, the driving wheels of the three wheel chains lose contact with the wall of the pipeline. On the contrary, the passive wheel of each wheel chain gains a contact with the wall. Thus, the robot can be retrieved from the pipeline by pulling a wire connected to the rear side of the robot. Fig. 7 and Fig. 8 detail such behavior.
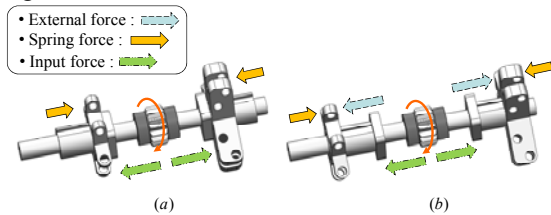
Fig. 6. The retrieval mode.

The driving mode is enabled when the active wheel of the wheel chain is located at the outer position as compared to position of the clutch wheel as shown in the Fig. 7(a). In this

mode, the robot can move because the active wheel driven by a motor contacts the inner surface of the pipeline. On the contrary, in Fig. 7(b), the driving mode is switched to the retrieval mode when the active wheel is located at the inner position. In this mode, the (passive) clutch wheel contacts the inner surface of the pipeline. Thus, a contact line between two idle wheels is formed. As a result, retrieval of the robot can be achieved. Moreover, if the power of the robot system is suddenly off, the mode is automatically changed to the retrieval mode due to the lower gear ratio of the axis drive motor that supports the external load exerted on the wheels. Thus, retrieval of the robot can be made easily.
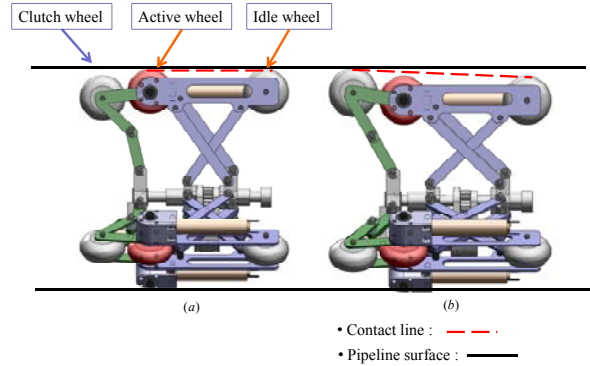
Fig. 7. The pipeline inspection robot system with a mechanical clutch : (a) driving mode, (b) clutch mode.

III. THE KINEMATICS OF MECHANISM

In this section, the positions of the clutch wheel, the active wheel, and the idle wheel will be derived in order to show the behavior of the clutch with respect to the input d_{In} caused by the main axis drive motor.

The wheel chain and clutch wheel parts can be represented as Fig. 8. Each wheel chain consists of two four-bar mechanisms and one five-bar mechanism. A four-bar mechanism consists of four revolute joints. The five-bar mechanism consists of four revolute joints and one prismatic joint. When applying an external force on the outer wheels, the height of wheel chain d_l is changed.

The center point p_{ecnt} of the main axis is stationary and the angle ψ_m between the main axis and a link of five-bar can calculated by using the law of cosine.
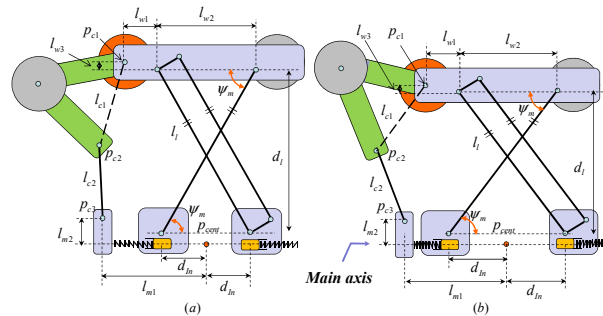
Fig. 8. The schematic diagram of working mode : (a) driving mode (b) retrieval mode.

Using the notation in Fig. 9, the law of cosines states that

$$c^2 = a^2 + b^2 - 2ab\cos\psi_m, \tag{1}$$

where $b = \dfrac{2d_{In} - l_{w2}}{2}$, $a = \dfrac{bl_l}{(l_{w2}+b)}$, and $c = \sqrt{a^2-b^2}$.

Rearranging (1) gives

$$\psi_m = \cos^{-1}\left(\frac{a^2+b^2-c^2}{2ab}\right). \tag{2}$$

The height d_l of the wheel chain is given by

$$d_l = l_l \sin\psi_m', \tag{3}$$

where $\psi_m' = \pi - \psi_m$.
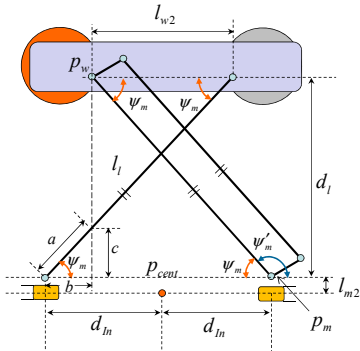
Fig. 9. The schematic diagram of the wheel chain.

In Fig. 10, the position of p_m is given as

$$x_{p_m} = l_{m1} + d_{In}, \; y_{p_m} = l_{m2} \tag{4}$$

and the position p_w is given as

$$x_{p_w} = x_{p_m} - l_l \cos\psi_m', \; y_{p_w} = y_{p_m} + d_l. \tag{5}$$

Also the position of p_{c1} (i.e., position of the driving wheel) is given as

$$x_{p_{c1}} = x_{p_w} - l_{w1}, \; y_{p_{c1}} = y_{p_w} + l_{w3}. \tag{6}$$
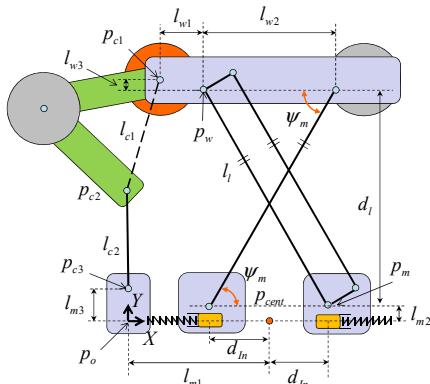
Fig. 10. The schematic diagram of the wheel chain and clutch wheel part.

The position analysis of the clutch wheel part is conducted by using the DYAD analysis [16]. In Fig. 11, the known parameters of 111 DYAD are l_{c1} and l_{c2}, and the unknown parameters of 111 DYAD are ψ_1 and ψ_2.

The length D is given as

$$D = \sqrt{(x_{p_{c3}} - x_{p_{c1}})^2 + (y_{p_{c3}} - y_{p_{c1}})^2} \tag{7}$$

and the angle β_i $(i=1,2)$ can be expressed as

$$\beta_i = a\cos\left(\frac{l_{c1}^2 - l_{c2}^2 - (-1)^i D^2}{2l_i D}\right) \tag{8}$$

and

$$\alpha = \tan^{-1}(v/u), \tag{9}$$

where

$$u = l_{c1}\cos\psi_1 - l_{c2}\cos\psi_2 = x_{p_{c3}} - x_{p_{c1}}$$
$$v = l_{c1}\sin\psi_1 - l_{c2}\sin\psi_2 = y_{p_{c3}} - y_{p_{c1}}. \tag{10}$$

The angles ψ_1 and ψ_2 can be expressed as

$$\psi_i = \alpha + TYPE(\beta_i), \; (i=1,2). \tag{11}$$
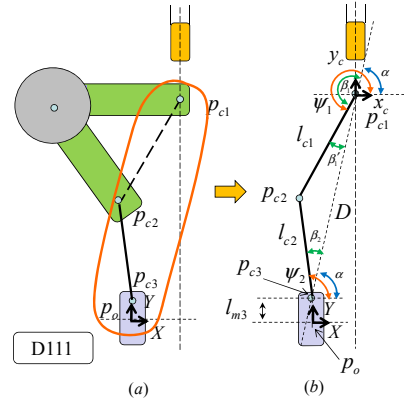
Fig. 11. The analysis of the 111 DAYD.

The positions of p_{c3} and p_{c2} are given as

$$x_{p_{c3}} = 0, \; y_{p_{c3}} = l_{m3}, \tag{12}$$

$$x_{p_{c2}} = x_{p_{c3}} + l_{c2}\cos\psi_2,$$
$$y_{p_{c2}} = y_{p_{c3}} + l_{c2}\sin\psi_2. \tag{13}$$

In Fig. 12, since $\triangle p_{c1}p_{c3}p_{c4}$ is a regular triangle, the position of p_{c4} (i.e., position of the clutch wheel) is given as follows

$$x_{p_{c4}} = x_{p_{c2}} + l_{c1}\cos\mu',$$
$$y_{p_{c4}} = y_{p_{c2}} + l_{c1}\sin\mu', \tag{14}$$

where

$$\gamma = 180° - (\beta_1 + \beta_2), \tag{15}$$
$$\zeta = 180° - \psi_2,$$
$$\mu = \gamma - \zeta, \; \mu' = \mu + 60°. \tag{16}$$
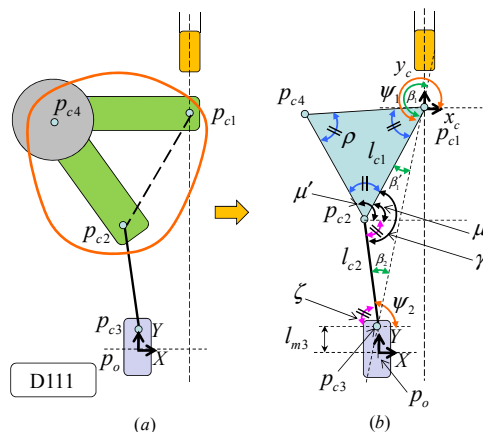
Fig. 12. The position analysis of the clutch wheel.

Based on the above position analysis, the behavior of the proposed kinematic model is tested through a numerical simulation using Matlab. Fig. 13 shows the simulation result of the wheel mechanism. When the input d_{In} is to the right, the position (p_{c4}) of the clutch wheel moves up, while the position (p_{c1}) of the wheel chain moves down. We can find out the suitable parameters of the linkage by using this kinematic simulation. Fig. 14 also shows the history of the angles ψ_1 and ψ_2 with respect to d_{In} for the D111 during this motion.
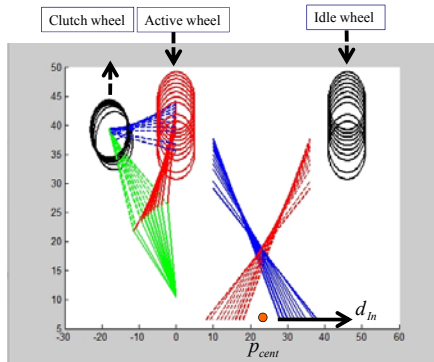
Fig. 13. The result of kinematic simulation.
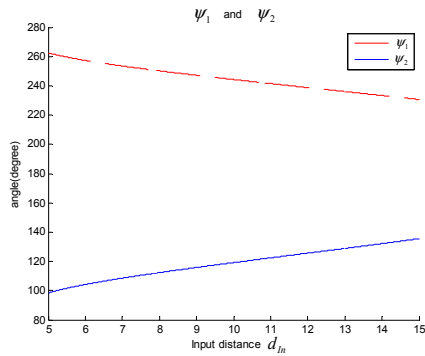
Fig. 14. History of ψ_1 and ψ_2.

IV. IMPLEMENTATION

A. Controller

The robot controller consists of a control box and a robot device as shown in the Fig. 15. The robot control is executed by a serial communication. In this system, we use two MCUs (Atmega128). One MCU calculates the angular velocity of the joystick interface and the linear velocity of the robot. The other MCU calculates the motor speed by producing a PWM signal. It can control all of the Micro DC motors. All the motor drives and MCU are integrated in the control box.

The view of the pipeline is provided to the user by using a Micro CMOS camera mounted in front of the robot body. This module makes it possible to inspect the condition inside the pipeline. The robot device equipped with a camera and a lighting device are shown in the Fig. 15.
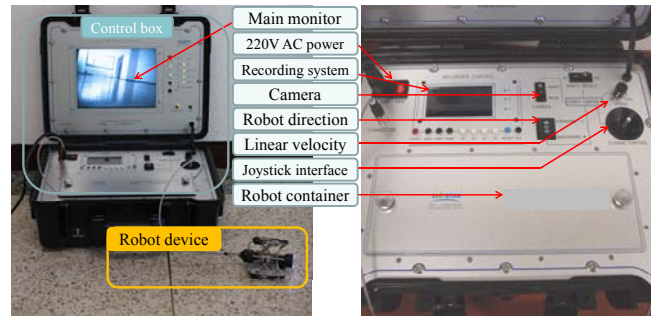
Fig. 15. The robot controller.

B. The robot device

The motors are embedded in the motor box of the wheel mechanism. The peak torque is 17.5 mNm. The Maxon re 6 and GP 6A gear head are chosen for this robot. Table I describes the specification of the motor and the gear head.

TABLE I
SPECIFICATION OF THE MOTOR(MAXON RE 6) AND THE GEARHEAD(GP 6A)

Specification	Value
Diameter	6 mm
Nominal voltage	6 v
Nominal speed	5320 rpm
Max. Continuous torque	0.321 mNm
Max. Continuous current	0.118 A
Gearhead reduction	221:1
Gearhead max. Continuous torque	30 mNm

Table II shows the specification of the robot. The length of the robot module is 80mm and the exterior diameter of the robot body changes from 90mm up to 110mm. The total length of the robot device including the camera and the lighting device is 122mm. And the weight of the robot is 189g. In this paper, a pipeline with diameter of 100 mm is employed as a test bed.

TABLE II
SPECIFICATION OF THE ROBOT

Specification	Tbot-100
Weight of the robot module	189g
Motor diameter	6mm
Length of the robot module	80mm
Total length of the robot (including camera and lightning module)	122mm
Exterior diameter	90-110mm
Linear speed	14cm/sec
Serial communication	15 M

V. EXPERIMENTAL RESULTS

A pipeline consisting of 6 elbows is employed as a test bed. The elbow is a commercial product. The total length of the test bed is 3m. Fig. 16 shows the test bed for the experimentation and Fig. 17 shows the driving and retrieval modes of the robot. Fig. 18 demonstrates that the pipeline inspection robot is able to go through several elbows and can be also retrieved successfully as shown in the Fig. 19.

Fig. 16. The test bed.

Thus, the performance of the proposed robot system could be verified through this experimentation. The attached video clip shows the experimental result.

VI. CONCLUSIONS AND FUTURE WORKS

We developed a new differential-drive type pipeline inspection robot with a linkage-type mechanical clutch for inspecting 100 mm pipelines. The behavior of the proposed kinematic model is tested through a numerical simulation. The performance of the proposed pipeline inspection robot system was verified through a variety of experiment under a test-bed environment. As the future work, optimal parameterization for the compression spring, gear ratio of the main axis drive motor, and kinematic dimension will be conducted.

REFERENCES

[1] T. Okada and T. Kanade, "A three-wheeled self-adjusting vehicle in a pipe, FERRET-1," *Int. J. Robot. Res.*, vol. 6, no. 4, pp. 60–75, 1987.

[2] H. T. Roman, B. A. Pellegrino, and W. R. Sigrist, "Pipe crawling inspection robots: An overview," *IEEE Trans. Energy Convers.*, vol. 8, pp. 576–583, Sept, 1993.

[3] W. Neubauer, "A spider-like robot that climbs vertically in ducts or pipes," in *Proc. IEEE/RSJ Int. Conf. Intell. Robots Syst.*, 1994, pp. 1178–1185.

[4] S. Hirose, H. Ohno, T. Mitsui, and K. Suyama, "Design of in-pipe inspection vehicles for _25, _50, _150 pipes," in *Proc. IEEE Int. Conf. Robot. Autom.*, 1999, pp. 2309–2314.

[5] J. Okamoto, Jr., J. C. Adamowski, M. S. G. Tsuzuki, F. Buiochi, and C.S. Camerini, "Autonomous system for oil pipelines inspection," *Mechatronics*, vol. 9, pp. 731–743, 1999.

[6] M. M. Moghaddam and A. Hadi, "Control and guidance of a pipe inspection-PIC," in *Proc. Int. Symp. Automations, Robotics*, 2005, pp. 11–14.

[7] T. Aoki and S. Hirose, "Study on the brake operation of bridle bellows," in *Proc. IEEE/RSJ Int. Conf. Intell. Robots Syst.*, 2007, pp. 40-45.

[8] P. Li, S. Ma, B. Li, and Y. Wang, "Design of a mobile mechanism possessing driving ability and detecting function for in-pipe inspection" in *Proc. IEEE Int. Conf. Robot. Autom.*, 2008, pp. 3992-3997.

[9] H. Lim, J. Y. Choi, Y. S. Kwon, E. J. Jung, and B.-J. YI, "SLAM in indoor pipelines with 15mm diameter," in *Proc. IEEE Int. Conf. Robot. Autom.*, 2008, pp. 2616–1619.

[10] M. M. Moghaddam and A. Hadi, "Control and guidance of a pipe inspection-PIC," in *Proc. Int. Symp. Automations, Robotics*, 2005, pp. 11–14.

[11] S. G. Roh, D. W. Kim, J. S. Lee, H. P. Moon, and H. R. Choi, "Modularized in-pipe robot capable of selective navigation inside of pipelines," in *Proc. IEEE/RSJ Int. Conf. Intell. Robots Syst.*, 2008, pp. 1724–1729.

[12] Y. S. Kwon and B.-J. Yi, "The kinematic modeling and optimal paramerization of an omni-directional pipeline robot," in *Proc. IEEE Int. Conf. Robot. Autom.*, 2009, pp. 1389-1394.

[13] Kuo-Tsai Chang, "Design and implementation of a piezoelectric clutch mechanism using piezoelectric buzzers industrial electronics and applications" in *Proc. IEEE Int. Conf. Industrial Electronics and applications*, 2007, pp. 2178-2183.

[14] H. Maekawa, Y. Gotoh, K. Sato, M. Enokizono, and K. Komoriya "Development and evaluation of a passively operating non-contact, load-responsive transmission," in *Proc. IEEE Int. Conf. Robot. Autom.*, 2004, pp. 4071-4078.

[15] S. G. Roh, D. W. Kim, J. S. Lee, H. P. Moon, and H. R. Choi, "In-pipe robot based on selective drive mechanism," *Int. Journal. Control, Automation, and Systems*, vol. 7, pp. 105-112, Feb. 2009.

[16] C.E. Benedict and D. Tesar, Model formulation of complex mechanisms with multiple inputs: Part II – The dynamic model. *ASME J. Mech. Design* Vol. 100, 1978, pp. 755–761.
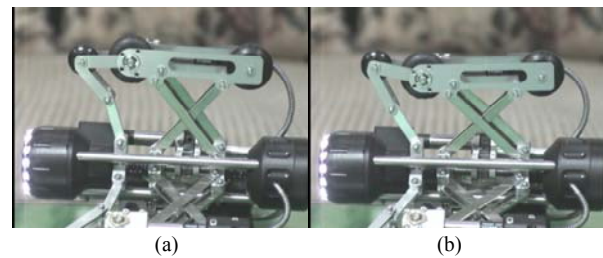
(a)   (b)
Fig. 17. The experimental result : (a) driving mode, (b) clutch mode.
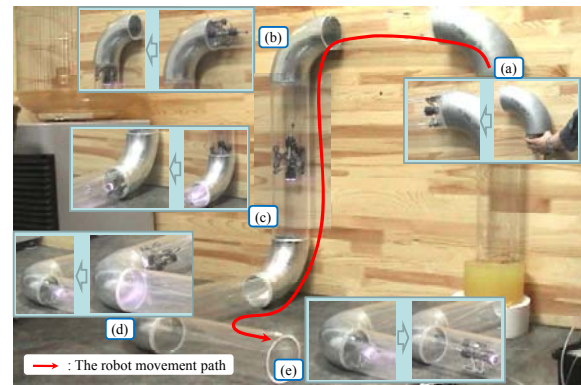
: The robot movement path
Fig. 18. The experimental result : navigation inside the pipeline.

(a)   (b)   (c)
(d)   (e)   (f)
Fig. 19. Retrieval of the robot.